Journal of Membrane Science 365 (2010) 319–328

Contents lists available at ScienceDirect

Journal of Membrane Science

journal homepage: www.elsevier.com/locate/memsci

A comparative study on the structure and performance of porous polyvinylidene fluoride and polysulfone hollow fiber membranes for CO_2 absorption

A.F. Ismail[a,b,*], A. Mansourizadeh[a,b]

[a] Advanced Membrane Technology Research Centre (AMTEC), Universiti Teknologi Malaysia, 81310 Skudai, Johor, Malaysia
[b] Department of Gas Engineering, Faculty of Petroleum and Renewable Energy Engineering, Universiti Teknologi Malaysia, 81310 Skudai, Johor, Malaysia

ARTICLE INFO

Article history:
Received 26 June 2010
Received in revised form 8 September 2010
Accepted 15 September 2010
Available online 22 September 2010

Keywords:
Hollow fiber membranes
Characterization
CO_2 absorption
Membrane contactor

ABSTRACT

Porous polyvinylidene fluoride (PVDF) and polysulfone (PSF) hollow fiber membranes were prepared via a wet spinning method. Glycerol was used as phase-inversion promoter additive in the spinning dopes. Cloud point diagrams of polymer/solvent–glycerol/water were obtained to study precipitation rate of the polymers solution. The membrane structure was compared in terms of morphology, gas permeation, critical water entry pressure, collapsing pressure, overall porosity, contact angle and mass transfer resistance. The cloud point diagrams confirmed a significant increase in the precipitation rate of the spinning dopes with addition of glycerol. The PSF membranes indicated more open cross-section structure with smaller pore sizes. However, the PVDF membranes illustrated an ultra thin outer skin layer with high permeability which resulted in significantly lower mass transfer resistance. Physical CO_2 absorption with distilled water was conducted through the gas–liquid membrane contactors. With addition of glycerol, the PVDF membrane demonstrated a structure with significantly higher CO_2 flux compared to the commercial asymmetric PVDF membrane. The CO_2 flux of 8.20×10^{-4} mol/m^2 s was achieved by using the absorbent flow rate of 310 mL/min in the shell side of the membrane module. Therefore, using an improved hollow fiber membrane structure can be a promising alternative for CO_2 absorption and separation through membrane contactors.

© 2010 Elsevier B.V. All rights reserved.

1. Introduction

Due to the rising emission of greenhouse gases and the related concerns over global warming and climate change, several techniques have been improved to remove CO_2 from the gas streams such as chemical and physical absorption, solid adsorption, cryogenic distillation and membrane gas separation [1]. However, to minimize overall environmental impacts and cost of CO_2 capture, the priority is given to the technologies with improved CO_2 removal efficiency. In recent years, membrane gas absorption process has attained considerable attention for CO_2 capture from the gas streams [2–7].

Indeed, the membrane contactors can overcome the disadvantages of conventional gas absorption devices due to certain characteristics such as high surface area per unit contactor volume, independent control of gas and liquid flow rates without any flooding, loading, weeping, foaming or entrainment problems, small size, having known gas–liquid interfacial area, being modular and easy to scale up or down [8]. By using a suitable membrane configuration such as a hollow fiber, fluids can be contacted on opposite sides of the membrane and the gas–liquid interface is formed at the mouth of each membrane pore. Mass transfer occurs by diffusion across the interface same as the traditional contacting equipment. Schematic of CO_2 absorption mechanism in porous membrane is given in Fig. 1. The porous membrane provides a flexible modular energy efficient device with a high gas–liquid contact area. The liquid absorbent offers a very high selectivity and driving force even at very low concentrations. However, it should be noted that not only the membrane adds an extra resistance to the mass transfer process compared to conventional contacting devices, but also wetting of the membrane can increase mass transfer resistance significantly. Hence, there is a need to prepare membranes with improved structure for gas absorption application. The essential properties of the membrane include high hydrophobicity with small pore size (high wetting resistance), high permeability (low mass transfer resistance) and excellent resistance to various chemical feed streams.

Hydrophobic polymeric materials such as polypropylene (PP), polyethylene (PE) and polytetrafluoroethylene (PTFE) cannot be dissolved in common solvents at low temperature. Therefore, the membranes are fabricated using stretching and thermal methods which generally provide symmetric structure with large pore sizes. On the other hand polyvinylidene fluoride (PVDF), the only hydrophobic polymer soluble in the organic solvents, has a small

* Corresponding author. Tel.: +60 07 5535 592; fax: +60 07 5581 463.
E-mail address: afauzi@utm.my (A.F. Ismail).

0376-7388/$ – see front matter © 2010 Elsevier B.V. All rights reserved.
doi:10.1016/j.memsci.2010.09.021

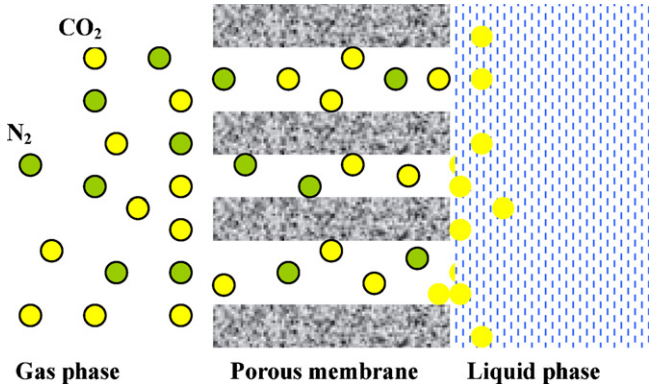

Fig. 1. Schematic of CO_2 absorption mechanism through porous membrane contactor.

critical surface tension about 25 dyn/cm that can limit the penetration of the coagulant (water) into the nascent membrane during the phase-inversion process. Therefore, slow solidification of the nascent membrane results in considerable difficulties in preparing porous PVDF hollow fiber membranes via phase-inversion method. Thus, introducing a strong non-solvent in the spinning dope can improve precipitation rate and results in porous membrane structure. It was reported that dry–wet spun PVDF hollow fiber membranes showed high gas permeability, good mechanical strength and excellent hydrophobicity, when water/LiCl, or 1-propanol/LiCl used as the additives in the spinning dopes [9]. Moreover, compared to distilled water as an additive in the PVDF polymer dope, glycerol and phosphoric acid showed larger pore size and higher value of molecular weight cut off (MWCO) that improved the membrane permeability and CO_2 absorption flux [10].

In addition, polysulfone (PSF) has been widely used as a membrane material due to its mechanical strength, thermo-stability, stability against chemicals and relative hydrophobicity. PSF is also an excellent material for spinning hollow fiber membranes with controlled pore sizes. In general, the non-solvent additives play an important role on phase-inversion rate of the polymer solution which governs the asymmetric membrane structure. In fact, fast solidification results in the membranes structure with high surface porosity and thin skin layer [11]. It was reported that addition of 5 wt.% polyvinylpyrrolidone (PVP) in 15 wt.% PSF solution improved the membrane permeate flux by factor of one. However, further increment of PVP in the solution resulted in delayed de-mixing of solvent–non-solvent and the permeate flux decreased [12]. In addition, it was found that 6 wt.% glycerol in 17 wt.% PSF spinning dope resulted in the membrane structure with improved CO_2 absorption flux compared to polyethylene glycol (PEG 200), ethanol and acetic acid as non-solvent additives [13].

Although a number of studies have been conducted on the preparation of porous PVDF and PSF hollow fiber membranes, an efficient study on improvement of porous membrane structure for CO_2 absorption, especially a comparative study on different membrane materials, is scarcely reported in the open literature. In this study, asymmetric PVDF and PSF hollow fiber membranes were prepared via a wet spinning process at the same conditions, where glycerol was used as a phase-inversion promoter additive in the polymers dopes. The precipitation rate of the polymers dope was studied using cloud point measurements. The morphology of the prepared membranes was compared via field emission scanning electron microscopy (FESEM) examination. The structure of the membranes was also characterized in terms of gas permeability, wetting resistance, mass transfer resistance, overall porosity and mechanical stability. In addition, the CO_2 absorption performance of the prepared membranes was compared through the gas–liquid membrane contactors.

Table 1
Spinning dopes composition and viscosity.

Spinning dope	D1	D2	D3	D4
PVDF (wt.%)	17	17	–	–
PSF (wt.%)	–	–	17	17
Glycerol (wt.%)	–	5	–	5
NMP (wt.%)	83	78	83	78
Viscosity (cp at 25 °C)	2080	2790	880	1590

2. Experimental

2.1. Materials

Commercial PVDF polymer pellets (Kynar® 740, Mn = 156,000) were supplied by Arkema Inc., Philadelphia, USA. PSF polymer pellets (Udel P-1700, Mn = 21,000) were supplied by Solvay Advance Polymers. 1-Methyl-2-pyrrolidone (NMP, >99.5%) (Merck) was used as solvent without further purification. Glycerol (anhydrous extra pure) was purchased from Merck and used as non-solvent additives in the polymer dopes. Methanol (GR grade, 99.9%) and n-hexane (99%) were used for post-treating the membranes before drying in atmosphere. Tap water was used as coagulation bath in all cases.

2.2. Measurement of cloud point

The polymer dopes were prepared using a constant 6 wt.% of the additives in the additive/solvent mixture with different polymer concentrations (range: 1–18 wt.%). The cloud point data were measured using titration method. Non-solvent (distilled water) was slowly added into the polymer dope under constantly agitation at 25 °C. In cases when local precipitation occurred, especially at higher polymer concentration, agitation was continued until the solution became homogeneous again. Then further addition of non-solvent was performed until the solution became permanently turbid (the titration end point). Consequently, the compositions at the cloud point were calculated by weight.

2.3. Fabrication of porous hollow fiber membranes

The polymers pellets were dried at 60 ± 2 °C in a vacuum oven for 24 h to remove moisture content. The spinning dopes were prepared at 60 °C using stirring until the solution became homogeneous. The composition and viscosity of the polymers solutions are given in Table 1. The polymers solutions were degassed for 24 h at room temperature before spinning. The hollow fiber spinning process by the dry-jet wet phase-inversion was explained elsewhere [14]. Table 2 lists the detailed spinning parameters.

The spun fibers were immersed in water for 3 days to remove the residual NMP and the additive. The prepared hollow fiber membranes were post-treated by the non-solvent exchange method

Table 2
Hollow fiber spinning conditions.

Dope extrusion rate (mL/min)	4.0
Bore flow rate (mL/min)	1.70
Bore composition (wt.%)	NMP/H_2O 80/20
External coagulant	Tap water
Air gap distance (cm)	0.50
Spinneret o.d./i.d. (mm)	1.20/0.55
Spinning dope temperature (°C)	25
External coagulant temperature (°C)	25

using methanol and n-hexane to minimize fiber deformation and pores collapse before drying at room temperature.

2.4. Field emission scanning electron microscopy examination

Field emission scanning electronic microscopy (FESEM) (ZEIZZ SUPRA 35VP) was used to examine the morphology of the spun PVDF and PSF hollow fiber membranes by the standard methods. The membrane samples were immersed in liquid nitrogen and fractured carefully. Then, the samples were dried in a vacuum oven and coated by sputtering platinum before testing. The FESEM micrographs of cross-section, internal surface, external surface and outer skin layer of the hollow fibers were taken at various magnifications.

2.5. Characterization of the hollow fiber membranes

The prepared porous membranes were characterized in terms of gas permeation, wetting resistance, overall porosity, mechanical stability and mass transfer resistance which are important parameters for gas absorption applications.

The overall gas permeation through the porous membrane can be considered as the combination of Poiseuille flow and Knudsen flow [15]. Hence, by using the gas permeation test and assuming cylindrical pores in the skin layer of the asymmetric membrane, the gas permeance, mean pore size and effective surface porosity can be calculated [13].

In the gas permeation test, pure N_2 was used as the test gas. The test apparatus was based on the volume displacement method [16]. The test module which contained two hollow fibers with the length of about 10 cm was used to determine N_2 permeance. The feed gas was supplied to the shell side of the module and the permeation rate was measured at 25 °C in the lumen side using soap-bubble flow meter. The upstream pressure was increased at 0.25×10^5 Pa intervals up to 2×10^5 Pa. The N_2 permeance of the membranes was then calculated according to the outer diameter of the hollow fibers.

Critical water entry pressure (CEP_w) test and contact angle measurement were conducted to estimate the wetting resistance of the prepared membrane. For measuring CEP_w, distilled water was fed into the lumen side of the hollow fiber membranes using a diaphragm pump. The pressure was slowly increased at 0.5×10^5 Pa interval. At each pressure interval, the membrane module was kept at the constant pressure for 30 min to check if any water droplet appeared in the outer surface of the fiber. CEP_w was considered as the pressure for the first water droplet on the outer surface of the hollow fiber. As for contact angle measurement, samples of the hollow fibers were dried in a vacuum oven at 60 ± 2 °C for 12 h. The sessile drop technique using a goniometer (model G1, Krüss GmbH, Hamburg, Germany) was used to measure contact angle of the outer surface of the hollow fibers. The contact angle values of each sample were measured at ten various positions of the sample and then averaged.

Collapsing pressure test was conducted to evaluate the mechanical stability of the hollow fiber membranes. During the gas permeation test, the upstream pressure in the module shell side was further increased at 0.5×10^5 Pa intervals. Collapsing pressure was considered as the pressure where a sudden decrease or increase in the permeate flow in lumen side appeared.

To measure the overall porosity of the membranes, five hollow fibers with the length of 50 cm were dried for 2 h at 105 °C in a vacuum oven and weighed. The overall porosity (ε_o) was calculated according to the commonly used method based on density measurements [17]:

$$\varepsilon_o\,(\%) = \left(1 - \frac{\rho_f}{\rho_p}\right) \times 100 \tag{1}$$

where ρ_f and ρ_p are the fiber and polymer density, respectively. The fiber density was calculated from the mass and volume ratio as:

$$\rho_f = \frac{4w}{\pi({d_o}^2 - {d_i}^2)L} \tag{2}$$

where L is the fiber length; w is fiber mass; d_i is the inner diameter and d_o is the outer diameter of the hollow fibers. The density of the PVDF and PSF polymers is 1.77 and 1.24 g/cm^3, respectively.

In addition, CO_2 absorption experiment was conducted in the gas–liquid membrane contactor to determine the membrane mass transfer resistance and CO_2 absorption flux. A total of 10 hollow fibers with the effective length of 15 cm were packed randomly in the stainless steel membrane module. Specifics of the gas–liquid membrane contactor module were given elsewhere [13]. Pure CO_2 was employed as the feed gas in the lumen side and distilled water as the liquid absorbent in the module shell side in contact with the outer skin layer of the hollow fibers. The gas flow rate was kept constant at 100 mL/min and the liquid flow rate was in the range of 40–320 mL/min. The gas side pressure was set at 1 bar where the liquid side pressure was maintained 0.2×10^5 Pa higher to avoid bubble formation in the liquid phase [18]. Using chemical titration method, the CO_2 concentration in the liquid outflow at various flow rates was measured to determine the CO_2 flux. Before taking the samples, all the experiments were carried out for 30 min to achieve a steady state condition. The flow diagram of the experimental setup is shown in Fig. 2.

The Wilson plot method [20] can be used to determine the membrane mass transfer resistance, quantitatively. For a hydrophobic hollow fiber membrane with gas filled pores, the overall mass transfer resistance (${K_o}^{-1}$) can be expressed by a resistance in series model [8,19]. In case of physical absorption with water, the gas side mass transfer resistance can be ignored due to the use of pure CO_2 as the feed gas stream. Therefore, it can be assumed that only the liquid and the membrane mass transfer resistances are contributed to the mass transfer process. The liquid mass transfer resistance is proportional to the liquid velocity ${U_l}^{-\alpha}$, where α is an empirical constant and U_l is the liquid velocity. A plot of ${K_o}^{-1}$ versus ${U_l}^{-\alpha}$ results in a straight line, which is known as Wilson plot. The value of α is selected as the one that provides the best straight line through the data points. The membrane mass transfer resistance is given by the intercept of the Wilson plot. The overall mass transfer coefficient (K_o) can be determined by mass balance across the length of the hollow fibers [4,5] as:

$$K_o = -\frac{Q_l}{A_i} \ln\left(1 - \frac{C_{l,o}}{HC_g}\right) \tag{3}$$

where Q_l is liquid flow rate (m^3/s), A_i is inner surface of hollow fibers or gas–liquid contact area (m^2); $C_{l,o}$ and C_g are liquid outlet and gas side concentration, respectively (mol/m^3); and H is Henry's law constant, which is 0.85 for CO_2–water system.

3. Results and discussion

3.1. Analysis of cloud point diagrams

In general, precipitation rate of polymer dope is an important parameter for fabricating porous membranes. Faster precipitation results in the membranes with high surface porosity and thin skin layer [9]. The addition of the non-solvent additives to the polymer dope was found to reduce the miscibility area of the system and increased the precipitation rate of the solutions [21]. In our previous study, it was found that using glycerol as an additive in the PSF spinning dope resulted in a significant increase in phase-inversion rate, which provided membranes with high sur-

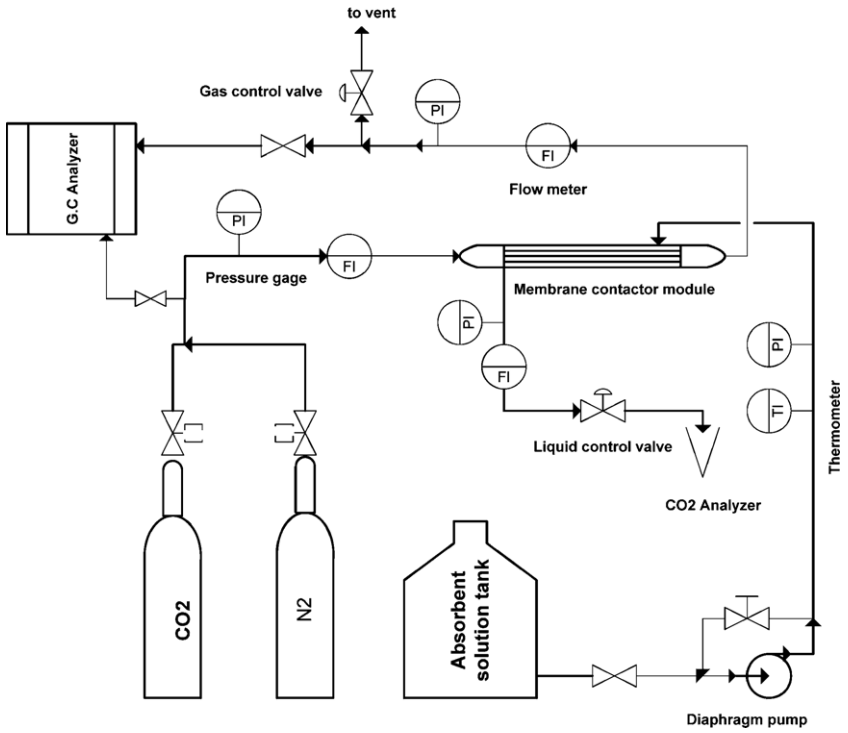

Fig. 2. Flow diagram of experimental setup for CO_2 absorption.

face porosity [13]. In present study, the cloud point diagrams of polymer/solvent–additive/water were obtained to investigate precipitation rate of the PVDF and PSF solutions.

The cloud points of the polymers solutions were obtained using titration method and the results are given in Fig. 3. As it can be seen, at high polymers concentration (over 10%), the PVDF solutions showed a slightly higher precipitation rate than PSF solutions which can be related to the different polymers properties. With addition of glycerol, the isothermal precipitation curves significantly shifted toward the polymer–solvent/additive axis. The cloud point results revealed that at 17 wt.% of PVDF concentration, water content required for precipitation of PVDF/NMP/glycerol solution was 1.37 wt.%. On the other hand, water content required for precipitation of PSF/NMP/glycerol solution was 3.28% of the solution, which shows a faster precipitation for the PVDF solution at the same polymer concentration. Indeed, a significant increase in the precipitation of the polymers dopes can be attributed to the strong non-solvent power of glycerol.

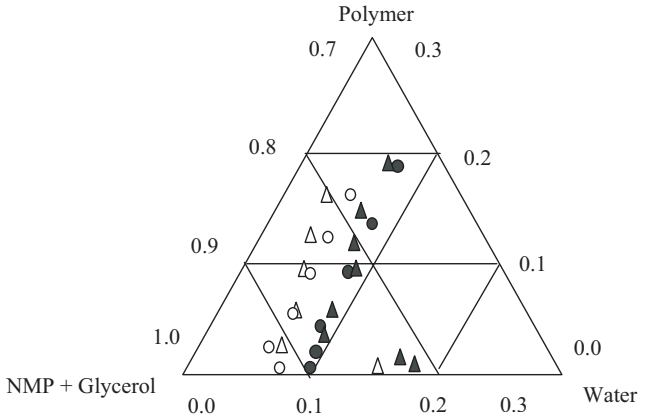

Fig. 3. Cloud point diagrams of polymer/solvent–additive/water system at 25 °C: (●) plain PSF; (▲) plain PVDF; (○) PSF/glycerol; and (△) PVDF/glycerol.

It can be concluded that the additive can reduce the solvent power and system tolerance for water, which results in promoting phase-inversion process. This phenomenon was expected to give porous membrane with improved surface porosity, which is favorable for gas absorption application.

3.2. Morphology of the hollow fiber membranes

The PVDF and PSF hollow fiber membranes were fabricated via a wet phase-inversion process at the same spinning conditions. Glycerol as a non-solvent additive was used in the polymers dopes in order to improve phase-inversion rate and prepare porous membranes. The morphology of the membranes was studied by FESEM to present cross-section, skin layer, outer surface and inner surface at different magnifications.

Fig. 4 shows the morphology of the prepared PVDF hollow fiber membranes. The membranes possess inner diameters from 650 to 670 μm, outer diameters from 890 to 950 μm and wall thickness from 120 to 150 μm. From the cross-section micrographs, the membranes structure consists of two kinds of morphologies: an outer finger-like layer with an ultra thin skin and an inner sponge-like layer without skin.

Generally, the asymmetric membrane structure during phase-inversion is controlled by the interactions between the polymer solution and the coagulant and the kinetic aspects during the phase-inversion process [22,23]. It must be mentioned that the addition of the non-solvent additives into the polymer dope decreases the thermodynamic miscibility of the dope solution, which results in enhancement of the liquid–liquid phase separation. On the other hand, the additives also increase the polymer dope viscosity, which decreases the mutual diffusion between the solvent and non-solvent [11]. Moreover, the increase in the polymer dope viscosity also shows the existence of stronger interactions among the components of the polymer dope [24]. Therefore, the membrane structure can be affected by a combination of the mentioned

aspects, which consequently impact the permeate performance of the membrane.

As it can be seen in Fig. 4a1 and b1, with addition of glycerol in the PVDF dope the finger-likes could not enlarge in the depth of the membrane structure compared to the plain PVDF membrane. The similar membrane morphology was observed for the addition of lithium chloride (LiCl) in the PVDF solution, where LiCl at high concentration (7.5%) suppressed microvoid formation [24]. Although, glycerol in the polymer dope increased the precipitation rate of the solution (see Fig. 3) which expected to provide an improved

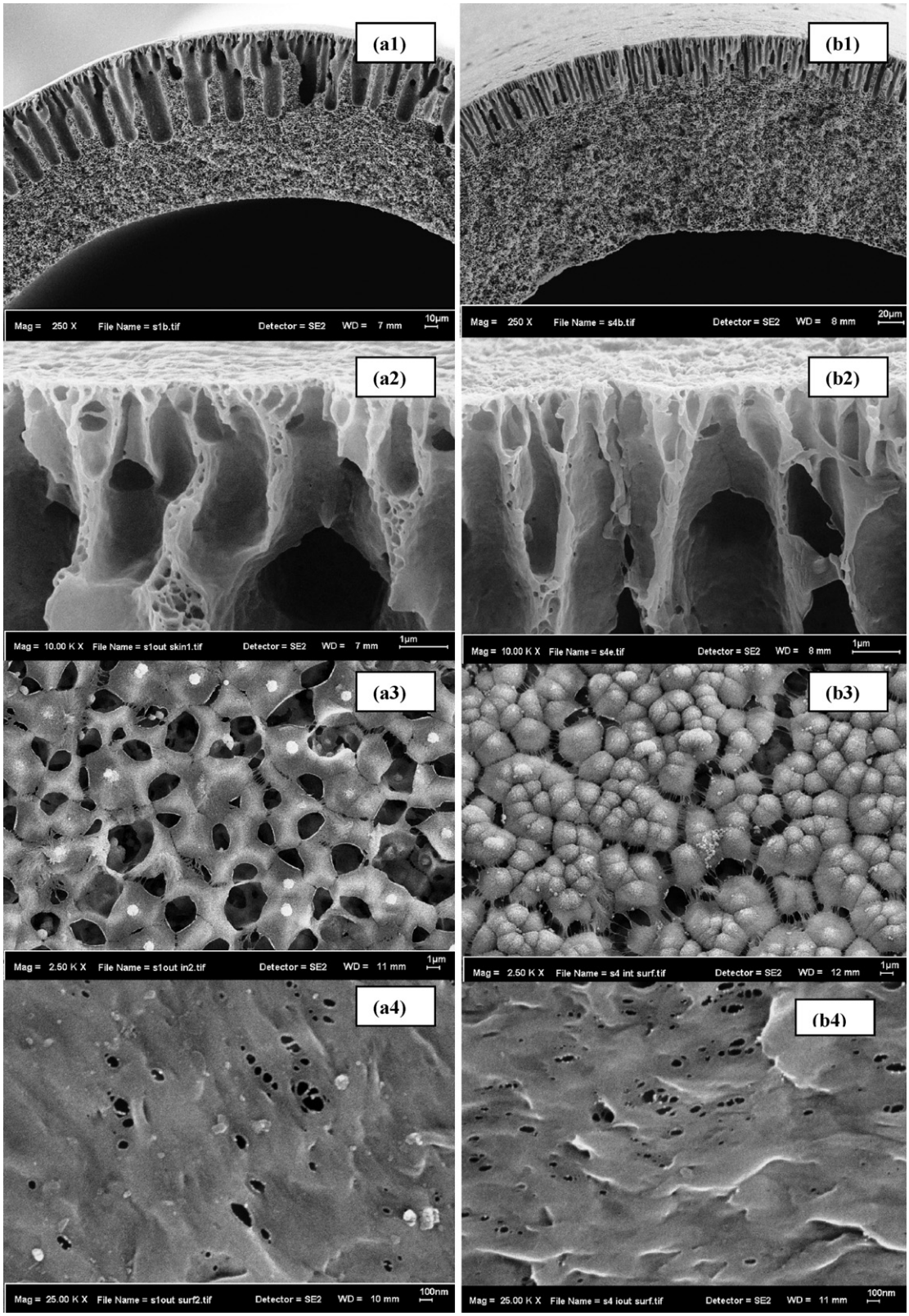

Fig. 4. FESEM morphology of the PVDF hollow fiber membranes: (a) without additive; (b) with glycerol; (1) cross section; (2) outer skin layer; (3) inner surface; and (4) outer surface.

finger-like structure, it seems that an increase in the viscosity of the solution played an important role in the morphology of the membrane. As for increased solution viscosity, there must be a specific interaction between glycerol, NMP and PVDF. It seems that –OH group of glycerol forms bridge-complexes with macromolecules fluorine or/and NMP carbonyl and nitrogen, and the complex formation potentially causes a decrease in macromolecules chains flexibility in the polymer dope and eventually increases the dope viscosity [25].

From Fig. 4b1, the formation of small finger-likes beneath outer skin layer can be related to the improved precipitation rate of the solution. The decrease in the mutual diffusion between solvent in polymer dope and non-solvent in coagulation bath due to the higher viscosity resulted in sponge-like sub-layer. However, for the polymer dope without glycerol with lower viscosity, the finger-likes were approximately two times larger than the polymer dope with glycerol.

In the wet phase-inversion process, the skin layer structure of an asymmetric membrane is likely to depend not only on the ratio of coagulant inflow to solvent outflow, but also on the diffusion rate of the non-solvent additive compared to the solvent [23,26]. Since the viscosity of the PVDF dope solutions is significantly higher than PSF solutions due to higher molecular weight, it seems that the solvent and/or non-solvent could not rapidly diffuse out of the polymer solutions. This phenomenon prevented an increase in the polymer concentration on the skin layer, and resulted in an ultra thin skin layer (around 80 nm thickness) with small pore sizes in the range of 10–150 nm visible at high magnification of FESEM (Fig. 4a2, b2, a4, and b4). Indeed, these properties are favorable for membrane gas absorption application.

In order to minimize the interaction between the spinning dopes and the bore fluid, the neutral bore composition can be adjusted by the cloud point phase diagram [27]. Therefore, using an aqueous solution of 80 wt.% NMP as the bore fluid for spinning of all the membranes resulted in the inner sponge-like layers without skin. In fact, an essentially neutral bore fluid can cause a very slow phase-inversion from the bore side relative to the coagulation bath, which can prevent skin layer formation [28,29]. As shown in Fig. 4a3 and b3, an open microporous structure was formed on the inner surface of the hollow fiber membranes, where the pore sizes were in the range of 0.3–6 μm.

Fig. 5 illustrates the morphology of the prepared PSF hollow fiber membranes. Although the membranes were spun at the same spinning conditions with the PVDF membranes, there are some differences in the membranes morphology that are mainly related to the phase-inversion behavior of the polymers dopes.

The PSF membranes possess inner diameters from 550 to 600 μm, outer diameters from 910 to 950 μm and wall thickness from 180 to 200 μm. From Fig. 5a1 and b1, the membranes cross-section consist of two layers: an outer finger-like layer with a thick skin and an inner sponge-like layer without skin and with some drop shape cavities.

With addition of glycerol to the PSF dope, the finger-likes became smaller same as the PVDF membranes, which can be attributed to the polymer dope viscosity. However, some drop shape cavities were appeared in the sponge-like layers compared to the PVDF membranes (Fig. 5a1 and b1). In fact, the formation of drop shape cavities in the inner layer can be associated to the slow phase-inversion because of the bore fluid composition. In slow solidification process, the wall between small droplets is difficult to be formed, thus many small droplets are combined to form larger droplets that generate drop shape cavities [28]. Moreover, as shown in Fig. 5b1, glycerol suppressed the cavities formation, which can be related to the enhanced solution viscosity.

From Fig. 5a2 and b2, the outer skin layers of the PSF membranes are thicker than those for the PVDF membranes. As discussed earlier, the mechanism of skin layer formation mainly depends on the mutual diffusion of solvent in polymer dope and non-solvent in coagulation bath. Since the viscosity of PSF dopes is lower than the PVDF dopes (Table 1), it can be said that faster out-diffusion of the solvent relative to the coagulant (water) resulted in the higher polymer concentration on the outer layer, which provided a relatively thick skin layer during the phase-inversion (100–200 nm). Consequently, an outer surface with very small pore sizes was obtained, where the pores could not be observed at high magnification of the FESEM (Fig. 5a4 and b4). In addition, an open microporous structure was also formed on the inner surface of the PSF hollow fiber membranes, which can be associated to the bore fluid composition.

3.3. Structure of the hollow fiber membranes

The PSF and PVDF materials were selected to prepare the asymmetric hollow fiber membranes with high permeability and wetting resistance. The characterization results of the hollow fiber membranes are given in Table 3.

Generally, overall porosity of the asymmetric membranes is related to the polymer dope composition, where higher polymer concentrations provide lower porosity and a higher amount of non-solvent additive results in higher porosity. In low polymer concentrations, the interaction between polymer molecules is low, and thus polymer aggregation results in open membrane structure with high porosity during the phase-inversion process. On the other hand, a sufficient amount of non-solvent additive in the polymer dope is responsible for initiation of polymer lean phase, which can provide a porous structure. As the results show, both PVDF and PSF membranes possess a good overall porosity, which can be a result of the low polymers concentration (17 wt.%) in the spinning dopes. Since only a small amount of glycerol as non-solvent (5 wt.%) was added to the polymers dopes, it seems that glycerol did not affect the membranes porosity.

The mechanical stability of the prepared membranes was examined in terms of collapsing pressure. Results show that the PSF membranes have a significantly higher mechanical stability than the PVDF membranes, which can be associated to the polymer structure and the membranes morphology. As discussed earlier, the PSF membranes possess an almost thick skin layer that can withstand higher collapsing pressure (Table 3). In addition, PSF is composed of phenylene units linked by three different chemical groups: isopropylidene, ether and sulfone. Each of the three linkages provides specific properties to the polymer, such as chemical resistance, temperature resistance and mechanical stability. On the other hand, the PVDF membranes possess ultra thin skin layer which results in lower mechanical stability. It is worth mentioning that the strong chemical resistance of fluoropolymers is directly linked to the strong bond between the carbon and fluorine atom within the polymer. Therefore, fully fluorinated fluoropolymers (PTFE) are typically more resistant to more chemicals and have higher temperature resistance than partially fluorinated fluoropolymers such as PVDF.

The contact angle measurement and the critical water entry pressure (CEP_w) test were conducted to examine the wetting resistance of the prepared membranes. In fact, long-term stable operation of the gas–liquid membrane contactor requires that the pores of membrane remain completely gas-filled over the prolonged periods of operational time. Using hydrophobic membranes with a high wetting resistance is a promising alternative for membrane gas absorption, which can minimize the mass transfer resistance. Since PVDF is well known as a hydrophobic material, its outer surface contact angle is higher than PSF membranes (Table 3). Moreover, the addition of glycerol in the polymers dopes resulted in the membranes with slightly higher contact angles. It can be said that glycerol could change the outer surface morphology of the

membranes. Glycerol is a low molecular weight additive, which can easily diffuse out from the nascent membranes during immersion and later washing process. In contrast, macromolecule weight additive such as PVP cannot completely wash out from the membrane structure and a trace of it in the membrane can seriously affect the membrane hydrophobicity.

All the prepared asymmetric membranes showed a relatively high CEP_w, which can be associated to the hydrophobicity and structure of the membranes. Since, all the membranes present nano-scale pore sizes, higher CEP_w of the PVDF membranes can be related to the membrane hydrophobicity. In addition, the membranes prepared by addition of glycerol demonstrated higher CEP_w

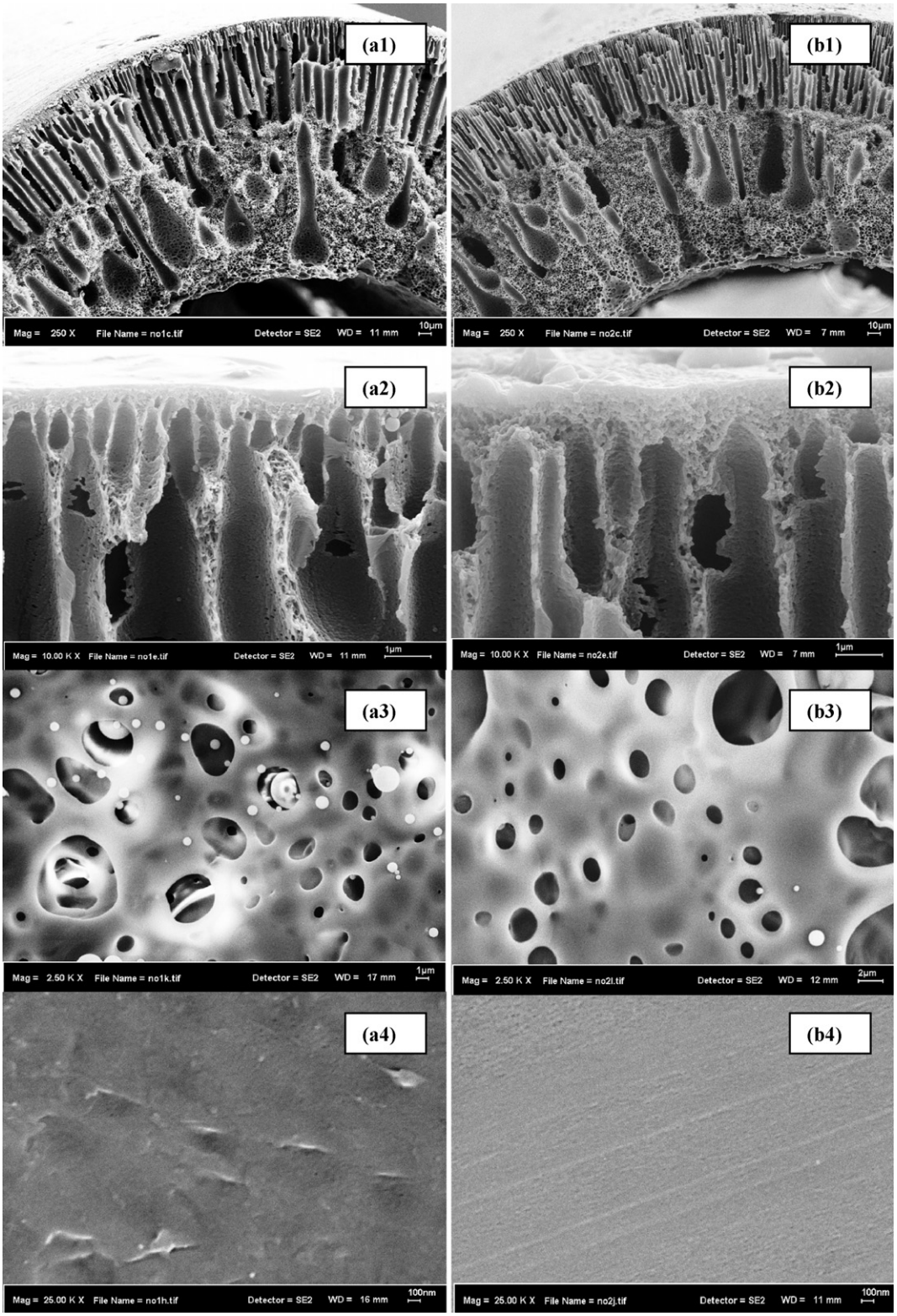

Fig. 5. FESEM morphology of the PSF hollow fiber membranes: (a) without additive; (b) with glycerol; (1) cross section; (2) outer skin layer; (3) inner surface; and (4) outer surface.

Table 3
Characteristics of prepared hollow fiber membranes.

Membrane	N_2 permeance at 1×10^5 Pa (10^{-3} cm^3/cm^2 s cmHg)	Mean pore size (nm)	Effective surface porosity ε/L_p (10^2 m^{-1})	CEP_w (10^5 Pa)	Collapsing pressure (10^5 Pa)	Overall porosity (%)	Contact angle (θ)
PVDF	15.50	7.80	2590	3	3.5	77	82 ± 1.80
PVDF + glycerol	11.60	9.60	1550	4.5	4	77	87 ± 1.03
PSF	3.70	6.10	836	2.5	7	76	64 ± 1.30
PSF + glycerol	3.40	7.30	603	3.5	7	76	69 ± 4.30

which is a result of sponge-like morphology. In fact, the sponge-like structure provides higher degree of tortusity, which does not allow water to penetrate through the membrane pores easily, meanwhile it can decline the membrane permeability [13,30]. Generally, critical entry pressure of the membranes is not only related to the membrane structure but also to the operating conditions and the liquid properties. The minimum liquid pressure required to penetrate in the membrane pores can be estimated by Laplace–Young equation [31]:

$$\Delta P = -\frac{2\gamma \cos\theta}{r_{p,\max}} \quad (4)$$

where γ is the surface tension of the liquid (N/m); θ is the contact angle between the membrane surface and liquid; and $r_{p,\max}$ is the maximum pore size of the membrane (m).

Therefore, it can be concluded that the membranes with smaller pore sizes, higher contact angle and sponge-like structure can withstand wetting during CO_2 absorption operation.

The values of N_2 permeance, mean pore size and effective surface porosity of the hollow fiber membranes were obtained from the gas permeation test (Table 3). The N_2 permeance of the PVDF membranes was significantly higher than the PSF membranes due to higher surface porosity and ultra thin skin layer. During the gas permeation test, N_2 permeance of the PVDF increased with pressure while it almost remained constant for the PSF membranes. This phenomenon indicates that Poiseuille and Knudsen flows govern the N_2 permeation through the PVDF and PSF membranes, respectively. Therefore, it can confirm the larger pore sizes of the PVDF membranes. Furthermore, with addition of glycerol, N_2 permeance of the membranes slightly decreased due to sponge-like structure with higher degree of tortusity.

3.4. CO_2 absorption performance of the membranes

Physical CO_2 absorption with distilled water was conducted in the gas–liquid membrane contactor in a continuous operation mode at 25 °C. As the skin layer of the membranes were in the outer surface, the liquid absorbent passed through the shell side in order to prevent wetting, and gas flowed counter-currently through the lumen side of the hollow fiber membranes. The mass transfer resistance and CO_2 absorption performance of the hollow fiber membranes were compared through the experimental analysis.

In order to measure the membranes mass transfer resistance, the Wilson plots of $1/K_o$ versus $U_l^{-0.53}$ were obtained as shown in Fig. 6. The α value of 0.53 was found to represent the best linear fit to the data of Wilson plot. A similar relationship of $1/K_o$ with $U_l^{-0.53}$ was correlated by Costello et al. [32] to describe the liquid flowing through the shell side of the hollow fiber membrane module. The intercept of the Wilson plots in Fig. 6 shows the membranes mass transfer resistance. As it can be seen, by increasing the absorbent velocity the overall mass transfer resistance considerably decreased. It confirms that the liquid phase resistance is dominant in the case of physical absorption. The results show that the membrane resistance contributed more to the overall resistance with a further increase in the absorbent velocity. This can be attributed to the decrease of the absorbent mass transfer resistance with the velocity.

With addition of glycerol in the polymers dope, the membranes resistance significantly decreased. Among the prepared membranes, the PVDF/glycerol hollow fiber membrane demonstrated the minimum value of mass transfer resistance, which mainly can be associated to its improved structure. On the other hand, the PSF membranes showed relatively high resistances due to the dense skin layer with lower permeability.

Fig. 7 shows the CO_2 absorption performance of the prepared membranes as a function of the absorbent velocity. It was observed that the CO_2 flux increased with an increase in the absorbents velocity for all the membranes. Indeed, by increasing the liquid velocity the boundary layer thickness around the fibers decreases. This phenomenon led to a reduction in the liquid mass transfer resistance and consequently could reduce CO_2 saturation in the boundary around the fibers.

From Fig. 6, although the plain PVDF membrane has the highest surface porosity, its relatively low CO_2 absorption flux could be a

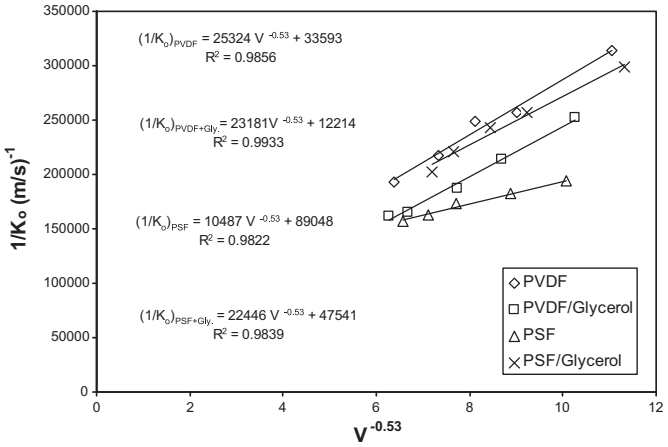

Fig. 6. Wilson plot of the hollow fiber membranes (pure CO_2–distilled water system).

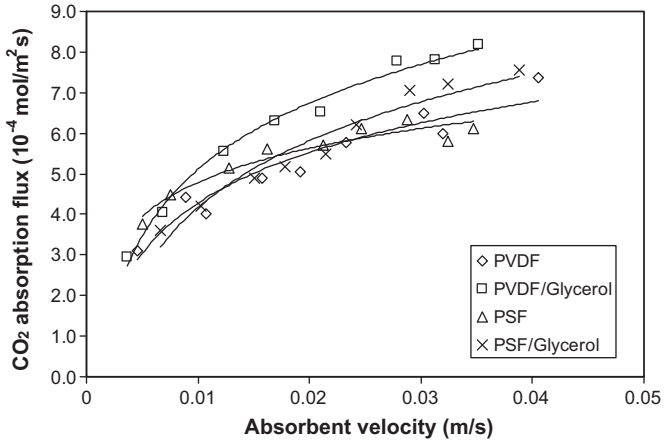

Fig. 7. CO_2 absorption performance of the hollow fiber membranes (pure CO_2–distilled water system).

result of lower wetting resistance. The CO_2 absorption rate of the plain PVDF membrane could not increase as fast as the other membranes with a greater increase in the absorbent flow rate. Therefore, it seems that its finger-like structure could not resist wetting during the operation and deteriorated the membrane performance.

The PVDF/glycerol membrane illustrated a significantly higher CO_2 flux than the other membranes. A maximum CO_2 flux of 8.20×10^{-4} mol/m^2 s was achieved at 0.035 m/s of the absorbent flow rate. At the same operating conditions, the CO_2 flux of the PVDF/glycerol membrane was compared with the commercial asymmetric PVDF hollow fiber membrane with mean pore size of 0.20 μm (Tianjin Motian Membrane Eng. & Tech. Co. Ltd, China). At 0.15 m/s of the absorbent velocity, the CO_2 flux of 6×10^{-4} mol/m^2 s was reported for the commercial membrane [10]. The prepared PVDF/glycerol membrane showed a CO_2 flux of approximately 36% higher than the commercial membrane flux at considerably lower absorbent velocity. Indeed, a noticeably higher CO_2 flux can be expected at the same absorbent velocity. This high CO_2 flux of the PVDF/glycerol membrane can be related to the improved membrane structure with low mass transfer resistance. As shown in Fig. 4, the membrane possess high surface porosity (high permeability) which provides high gas–liquid contact area for mass transfer process. The ultra thin outer skin layer and inner skinless layer of the membrane can also minimize the mass transfer resistance. In addition, its finger-like/sponge-like structure can resist wetting and eventually deterioration of the CO_2 flux during the operation. It was found by Wang et al. [33] that the overall mass transfer resistance was drastically increased even if the membrane pores were 5% wetted.

As for the PSF membranes, although glycerol in the PSF spinning dope could improve the membrane structure and reduce the resistance considerably, the resulted CO_2 flux was approximately 12% lower than the PVDF/glycerol membrane at 0.035 m/s of the absorbent velocity. This lower flux can be related to the lower surface porosity and smaller pore sizes of the membrane. Moreover, the dense skin layer of the PSF membranes resulted in the relatively high mass transfer resistances.

4. Conclusion

Porous PVDF and PSF hollow fiber membranes were fabricated using wet phase-inversion process. In order to improve the membranes structure for CO_2 absorption, glycerol was introduced to the polymer dopes as a non-solvent additive. An aqueous solution of 80 wt.% NMP was used as the bore fluid to provide inner skinless structure hollow fibers (low mass transfer resistance). The prepared membranes were characterized in terms of gas permeability, wetting resistance, overall porosity, mechanical stability and mass transfer resistance, which are important parameters for gas absorption applications. The phase-inversion behavior of the polymers dopes was also studied using the cloud point diagrams. The same membrane contactor module was used to compare CO_2 absorption performance of the prepared PVDF and PSF membranes. The cloud point diagrams confirmed a significant increase in the precipitation rate of the spinning dopes with the additive. From FESEM examination, the PVDF membranes showed an ultra thin outer skin with a high surface porosity. Results of the gas permeation test revealed that the PSF membranes possess significantly lower permeability with smaller pore sizes. In addition, the PVDF membranes showed higher hydrophobicity in terms of contact angle and critical water entry pressure, which can withstand wetting during CO_2 absorption. With addition of glycerol, the asymmetric PVDF membrane showed the highest CO_2 absorption flux among the prepared membranes. At the absorbent velocity of 0.035 m/s, the CO_2 flux of 8.20×10^{-4} mol/m^2 s was achieved, which was significantly higher than the CO_2 flux of the asymmetric commercial PVDF membrane. Therefore, it can be concluded that the hydrophobic PVDF hollow fiber membrane with improved structure can be a promising alternatives for CO_2 absorption and separation through gas–liquid membrane contactors.

Acknowledgement

The authors gratefully acknowledge the financial support from the Ministry of Science, Technology and Environment, Malaysia, with the grant number of 03-01-06-SF0282.

References

[1] P. Riemer, Green gas mitigation technologies, an overview of the CO_2 capture, storage and future activities of the IEA Greenhouse Gas R&D Programme, Energy Convers. Manag. 37 (1996) 665–670.
[2] S.A.M. Marzouk, M.H. Al-Marzouqi, M.H. El-Naas, N. Abdullatif, Z.M. Ismail, Removal of carbon dioxide from pressurized CO_2–CH_4 gas mixture using hollow fiber membrane contactors, J. Membr. Sci. 351 (2010) 20–27.
[3] S.H. Yeon, B. Sea, Y.L. Park, K.H. Lee, Determination of mass transfer rates in PVDF and PTFE hollow fibers membranes for CO_2 absorption, Sep. Sci. Technol. 38 (2003) 271.
[4] A. Mansourizadeh, A.F. Ismail, T. Matsuura, Effect of operating conditions on the physical and chemical CO_2 absorption through the PVDF hollow fiber membrane contactor, J. Membr. Sci. 353 (2010) 192–200.
[5] V.Y. Dindore, D.W.F. Brilman, P.H.M. Feron, G.F. Versteeg, CO_2 absorption at elevated pressures using a hollow fiber membrane contactor, J. Membr. Sci. 235 (2004) 99–109.
[6] D. deMontigny, P. Tontiwachwuthikul, A. Chakma, Using polypropylene and polytetrafluoroethylene membranes in a membrane contactor for CO_2 absorption, J. Membr. Sci. 277 (2006) 99–107.
[7] K. Simons, K. Nijmeijer, M. Wessling, Gas–liquid membrane contactors for CO_2 removal, J. Membr. Sci. 340 (2009) 214–220.
[8] A. Gabelman, S.T. Hwang, Hollow fiber membrane contactors, J. Membr. Sci. 159 (1999) 61–106.
[9] D. Wang, K. Li, W.K. Teo, Porous PVDF asymmetric hollow fiber membranes prepared with the use of small molecular additives, J. Membr. Sci. 178 (2000) 13–23.
[10] S. Atchariyawut, C. Feng, R. Wang, R. Jiraratananon, D.T. Liang, Effect of membrane structure on mass-transfer in the membrane gas–liquid contacting process using microporous PVDF hollow fibers, J. Membr. Sci. 285 (2006) 272–281.
[11] M. Mulder, Basic Principles of Membrane Technology, Kluwer Academic Publishers, The Netherlands, 2003.
[12] M.J. Han, S.T. Nam, Thermodynamic and rheological variation in polysulfone solution by PVP and its effect in the preparation of phase inversion membrane, J. Membr. Sci. 202 (2002) 55–61.
[13] A. Mansourizadeh, A.F. Ismail, Effect of additives on the structure and performance of polysulfone hollow fiber membranes for CO_2 absorption, J. Membr. Sci. 348 (2010) 260–267.
[14] A.F. Ismail, I.R. Dunkinb, S.L. Gallivanb, S.J. Shilton, Production of super selective polysulfone hollow fiber membranes for gas separation, Polymer 40 (1999) 6499–6506.
[15] J.M.S. Henis, M.K. Tripodi, Composite hollow fiber membranes for gas separation: the resistance model approach, J. Membr. Sci. 8 (1981) 233–246.
[16] A.F. Ismail, S.N. Kumari, Potential effect of potting resin on the performance of hollow fibre membrane modules in a CO_2/CH_4 gas separation system, J. Membr. Sci. 236 (2004) 183–191.
[17] F. Tasselli, J.C. Jansen, F. Sidari, E. Drioli, Morphology and transport property control of modified poly (ether ether ketone) (PEEKWC) hollow fiber membranes prepared from PEEKWC/PVP blends: influence of the relative humidity in the air gap, J. Membr. Sci. 255 (2005) 13–22.
[18] A. Malek, K. Li, W.K. Teo, Modeling of microporous hollow fiber membrane modules operated under partially wetted condition, Ind. Eng. Chem. Res. 36 (1997) 784–793.
[19] A. Mansourizadeh, A.F. Ismail, Hollow fiber gas–liquid membrane contactors for acid gas capture: a review, J. Hazard. Mater. 171 (2009) 38–53.
[20] E.E. Wilson, A basis for rational design of heat transfer apparatus, Trans. ASME 37 (1915) 47–82.
[21] M.L. Yewo, Y.T. Liu, K. Li, Isothermal phase diagrams and phase-inversion behavior of poly(vinylidene fluoride)/solvents/additives/water systems, J. Appl. Polym. Sci. 90 (2003) 2150–2155.
[22] W.J. Koros, G.K. Fleming, Membrane-based gas separation, J. Membr. Sci. 83 (1993) 1–80.
[23] D. Wang, K. Li, W.K. Teo, Polyethersulfone hollow fiber gas separation membranes prepared from NMP/alcohol solvent systems, J. Membr. Sci. 115 (1996) 85–108.
[24] E. Fontananova, J.C. Jansen, A. Cristiano, E. Curcio, E. Drioli, Effect of additives in the casting solution on the formation of PVDF membranes, Desalination 192 (2006) 190–197.

[25] I.M. Wienk, R.M. Boom, M.A.M. Beerlage, A.M.W. Bulte, C.A. Smolders, H. Strathmann, Recent advance in the formation of phase inversion membranes made from amorphous or semi-crystalline polymers, J. Membr. Sci. 113 (1996) 361–371.
[26] T.H. Young, L.W. Chen, A two step mechanism of diffusion-controlled ethylene vinyl alcohol membrane formation, J. Membr. Sci. 57 (1991) 69–81.
[27] D.W. Wallace, C.S. Bickel, W.J. Koros, Efficient development of effective hollow fiber membranes for gas separations from novel polymers, J. Membr. Sci. 278 (2006) 92–104.
[28] A. Xu, A. Yang, S. Young, D. deMontigny, P. Tontiwachwuthikul, Effect of internal coagulant on effectiveness of polyvinylidene fluoride membrane for carbon dioxide separation and absorption, J. Membr. Sci. 311 (2008) 153–158.
[29] H.J. Kim, R.K. Tyagi, A.E. Fouda, K. Jonasson, The kinetic study for asymmetric membrane formation via phase-inversion process, J. Appl. Polym. Sci. 62 (1996) 62–629.
[30] A. Mansourizadeh, A.F. Ismail, M.S. Abdullah, B.C. Ng, Preparation of polyvinylidene fluoride hollow fiber membranes for CO_2 absorption using phase-inversion promoter additives, J. Membr. Sci. 355 (2010) 200–207.
[31] A.C.M. Franken, J.A.M. Nolten, M.H.V. Mulder, D. Bargeman, C.A. Smolders, Wetting criteria for the applicability of membrane distillation, J. Membr. Sci. 33 (1987) 315–328.
[32] M.J. Costello, A.G. Fane, P.A. Hogan, R.W. Schofield, The effect of shell side hydrodynamics on the performance of axial flow hollow fiber modules, J. Membr. Sci. 80 (1993) 1–11.
[33] R. Wang, H.Y. Zhang, P.H.M. Feron, D.T. Liang, Influence of membrane wetting on CO_2 capture in microporous hollow fiber membrane contactors, Sep. Purif. Technol. 46 (2005) 33–40.